JOURNAL OF CATALYSIS **171,** 313–319 (1997)
ARTICLE NO. CA971800

Surface Chemistry of Supported Chromium Oxide on Lanthanum Carbonate

Manh Hoang,*,[1] Anthony E. Hughes,* Joseph F. Mathews,† and Kerry C. Pratt‡

*Division of Materials Science and Technology, CSIRO, Private Bag 33, Rosebank MDC, South Clayton, Victoria 3169, Australia;
†Department of Chemical Engineering, Monash University, Clayton, Victoria 3168, Australia;
and ‡Swinburne University of Technology, Hawthorn, Victoria 3122, Australia

Received April 7, 1997; accepted June 4, 1997

The surface chemistry of supported chromium oxide on lanthanum carbonate has been studied by TPD, FTIR, XPS, and electrophoretic measurement techniques. The active center for the oxidative dehydrogenation of isobutane to isobutylene was identified as a chromate species bound to the surface of lanthanum carbonate. This species was formed as a result of interaction between chromium oxide and lanthanum carbonate surface through CO_2 elimination. FTIR and XPS experiments have confirmed a complete reversibility of active sites during reduction–oxidation.

INTRODUCTION

Supported chromium oxides are well known to possess high activities for hydrogenation, isomerization of olefins, and dehydrogenation of alkanes (1, 2). The industrial importance of chromium-based catalysts has led to a large number of fundamental studies relating their catalytic and specific surface properties. The catalytic properties of this system are due to the surface chromium species formed as the result of chromium–support interaction. The commercial catalysts consist of the metal supported on high surface area alumina, silica, or on spinel-type materials such as Zn or Mg aluminate.

Supported chromium oxide is active for the selective oxidation of hydrocarbons. For example, chromium supported on silica has been found to be effective for the oxidation of methane to methanol (3). The catalyst comprises surface oxide chromates in which the chromium is chemically bound to the oxygen of the catalyst support.

Active carbon doped with chromium oxide and other redox-active transition metals have been reported to exhibit high activity and selectivity for the oxidative dehydrogenation of ethylbenzene to styrene (4).

The catalytic properties of supported chromium catalysts are thus strongly affected by the acidity/basicity of the oxide support (2). The reactivities of the surface chromium oxide species are controlled primarily by metal–support interactions, as the bulk oxides such as CrO_3 or Cr_2O_3 are believed to be inactive phases (5). In a Raman spectroscopic study, Kim and Wachs revealed that polymeric chromium oxide species possessing two terminal $Cr{=}O$ bonds preferentially exist on Al_2O_3, TiO_2, ZrO_2, and Nb_2O_5 supports and isolated chromate species with two $Cr{=}O$ bonds predominate on SiO_2. With MgO, nonstoichiometric compounds, $Mg_x(CrO_4)_y$, was found.

In another study, supported chromium oxide on lanthanum carbonates have been found to be active and selective for oxidative dehydrogenation of isobutane to isobutylene (6). This paper extends our study into the surface chemistry of this catalyst.

EXPERIMENTAL

Catalyst Preparation

The carbonate precursor was prepared by the dropwise addition of a solution of a mixture of $La(NO_3)_3 \cdot 6H_2O$ and $Cr(NO_3)_3 \cdot 9H_2O$, in the appropriate mole ratios, to a stirred solution of NH_4HCO_3. The resultant hydrogel was separated by centrifugation and washed with water and then with acetone. The product was first dried at room temperature in an air stream and then at 110°C in air for 4 h. The final catalyst was obtained by calcination at 300°C in air for 2 h.

Characterization

Infrared spectroscopy. FTIR spectra were recorded on a Mattson Cygnus 100 spectrophotometer. For general characterization, the IR spectra were taken as KBr disk. *In situ* IR studies were carried out in a specially designed optical cell which can be heated to 400°C under controlled atmosphere. The cell consists of a heating zone, constructed of silica glass and the remainder of the Pyrex glass. The cell was fitted with 30-mm-diameter KBr windows and valves for gas sampling and then mounted on a vacuum system which can maintain pressure of approximately 10^{-3} Torr. The IR spectra were recorded on thin, self-supporting wafers. Prior

---

[1] To whom correspondence should be addressed.

0021-9517/97 $25.00

to every sample measurement, a background spectrum was measured.

Surface area measurements. Surface areas were measured by nitrogen adsorption at −196°C using a Carlo Erba Sorbtomatic Series 1800 instrument.

Temperature-programmed decomposition (TPD). Details of the TPD apparatus used in this study have been reported previously (7). The reactor consists of a 6-mm o.d. silica tube with a silica frit at the center, heated by a temperature-programmable furnace. A He flow used as carrier gas was passed over the catalyst, while the temperature was programmed linearly to a designed temperature at a rate of 20°C/min. Water was removed by a trap working at dry ice temperature and the exit gas was analyzed by a thermal conductivity detector.

Thermogravimetric analysis (TGA). TGA was performed using a Stanton-Redcroft STA-700, simultaneous thermal analyzer. Nitrogen was used as a carrier gas.

X-ray photoelectron spectroscopy (XPS). XPS was carried out in a Vacuum Generators ESCALAB using a Mg anode (1256.6 eV) operated at 200 W in a chamber pressure of approximately 10^{-9} Torr. The spectrometer was calibrated using the photoelectron peaks from clean Cu and Au metals, namely, Cu2$p_{3/2}$, Cu3p and Au4$f_{7/2}$ with binding energy values of 932.6, 75.3, and 84.0 eV, respectively. The spectrometer was operated at 30 eV pass energy giving a halfwidth at half maximum for Ag3$d_{5/2}$ of 1.1 eV.

The catalyst oxidation/reduction studies were carried out *in situ* at 250°C using 1% O_2/He mixture for oxidation and pure isobutane for reduction at a pressure of 30 to 50 kPa. All XPS measurements were performed on catalyst disks pressed from loose powder. The gas flow rate was approximately 15 cc/min.

The Cr2p spectra were fitted with doublet Gauss/Lorentz product functions (9.7 eV separation and 0.52 relative intensity) after Shirley background subtraction. The doublet accounts for the Cr2$p_{3/2}$ and Cr2$p_{1/2}$. For some spectra it was evident that two species were present; hence, two components were fitted to these Cr2p spectra. The significance of fitting two as opposed to one component was determined statistically using reduced χ^2 and the Q-factor (8). The Q-factor is the integral of the χ^2 distribution and should be close to 0.5 for maximum statistical significance.

Electrophoretic measurements. Zeta potential measurements were performed on a Malvern Zetasizer-4. The samples were first prepared by ultrasonically suspending of 25 mg of catalyst in 50 ml of 10^{-3} *M* KCl solution. The pH was then adjusted using either dilute HCl or KOH solutions.

The value of the Zeta potential, determined by measurement of electrophoretic mobility, has been used for determination of the apparent surface fraction of the support that is covered by the supported phase (9–12). Zero point of charge (ZPC) of mixtures and isoelectric point (IEP) of pure components are related as

$$\mathrm{ZPC} = \sum_i X_i (\mathrm{IEP})_i,$$

where X_i is the mole fraction of each component.

Although there is a remarkable difference in composition between the surface and the bulk, the electrophoretic measurements have been shown to be an appropriate surface technique when applied to catalytic systems.

The "appearance surface coverage" (ASC) of a supported catalyst is calculated based on the fact that the zero point of charge of the catalyst normally falls between the isoelectric points of support and the supported component. According to Gil-Llambia *et al.* (9, 10). The ASC can be calculated by the equation

$$\mathrm{ACS} = \frac{(\mathrm{IEP_s} - \mathrm{ZPC})M_\mathrm{s}^{-1}}{\left(M_\mathrm{m}^{-1} - M_\mathrm{s}^{-1}\right)(\mathrm{ZPC} - \mathrm{IEP_s}) + (\mathrm{IEP_s} - \mathrm{IEP_m})M_\mathrm{m}^{-1}} \times 100,$$

where subscripts "s" and "m" represent support and supported material and M_s and M_m are the molecular weights of the support and supported material, respectively.

RESULTS AND DISCUSSIONS

Temperature-Programmed Decomposition

Active phase and support interaction. A catalyst consisting of 50 mol% Cr_2O_3 supported on $La_2(CO_3)_3$ was selected for investigation. Under the above precipitation conditions, the catalyst precursor was precipitated as a mixture of $NH_4Cr(OH)_2CO_3$ and $La_2(CO_3)_3$ (6). The TGA of a $NH_4Cr(OH)_2CO_3$ sample prepared under the same conditions shows a complete decomposition at 300°C to Cr_2O_3. The catalyst was thus first calcined in air at 300°C for 2 h. As $NH_4Cr(OH)_2CO_3$ is no longer stable at this temperature, the active chromium species starts to form on the catalyst surface. In fact, the temperature-programmed decomposition of calcined material shows only the decomposition of lanthanum carbonate as can be seen in Fig. 1. The first step peaking at 480°C corresponds to the formation of dioxycarbonate, $La_2O_2CO_3$ (7), and the second step reached a maximum rate at about 600–650°C. The temperature of this peak is considerably lower than that for the further decomposition of $La_2O_2CO_3$ to La_2O_3 (7) (Fig. 1), indicating that the interaction between chromium oxide and lanthanum carbonate has started. The formation of $LaCrO_3$ at temperatures >600°C was confirmed by XRD.

Infrared Spectroscopy

Formation of active phase. There has been a number of studies on the formation of surface chromate using

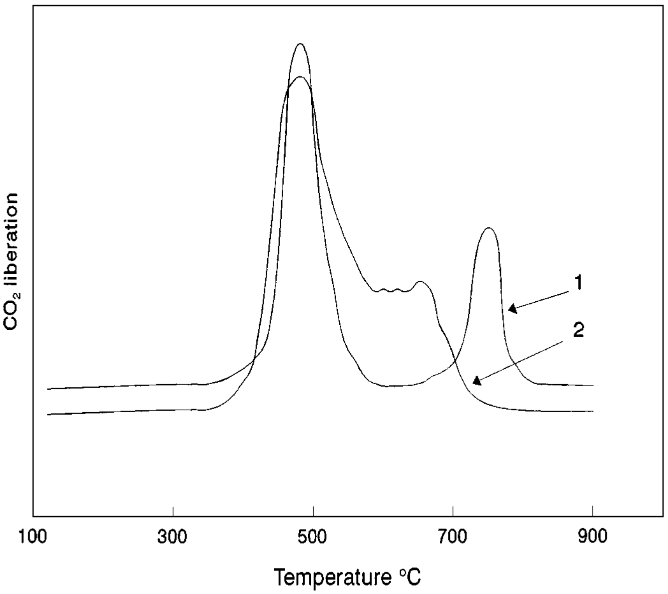

FIG. 1. Temperature-programmed decomposition of (1) $La_2(CO_3)_3$ and (2) $Cr_2O_3/La_2(CO_3)_3$.

the FTIR technique, and IR spectra for the Cr=O region have been reported. The IR spectra of supported chromium oxide on alumina, zirconia, titania, and silica are characterized by the presence of two groups of infrared bands: a high-frequency group consisting of bands in 1000–1050 cm^{-1} region assigned to isolated or nonisolated Cr(V)=O species and a lower frequency group consisting of bands in 850–950 cm^{-1} region attributable to Cr(VI) polychromate or dichromate species, as they alone absorb in that region (13–15). The formation of surface chromium species is influenced by the nature of the support, particularly the acidity/basicity as well as the reducibility. The reactivity of the surface chromium oxide species was found to depend on the surface oxide–support interaction. It is well recognized that IR spectroscopy can provide surface structural information on supported metal oxide catalysts. The surface chemistry of supported chromium oxide catalysts has been studied by a number of authors using FTIR. Kim and Wachs (2) have proposed from Raman and IR spectroscopic studies that on the surface of TiO_2, ZrO_2, Nb_2O_5, and Al_2O_3 supports that there exist polymeric chromium oxide species possessing two terminal Cr=O bonds.

For supported chromium oxide/lanthanum carbonate, after activation in air at 240°C, the IR spectrum of 10% chromium oxide loading catalyst features an intense broad band at 908 cm^{-1} and a very small shoulder at 1000 cm^{-1}. The sharp band at 1075 cm^{-1} is attributed to $La_2(CO_3)_3$ (Fig. 2). IR bands below 850 cm^{-1} could not be detected due to the increase in the background of the spectrum. In comparison to the data reported in the literature, the appearance of the band at 908 cm^{-1} strongly suggests the formation of surface chromate species. IR absorption in the chromium–oxygen overtone stretching region could not be detected because of strong lanthanum carbonate absorption in this region.

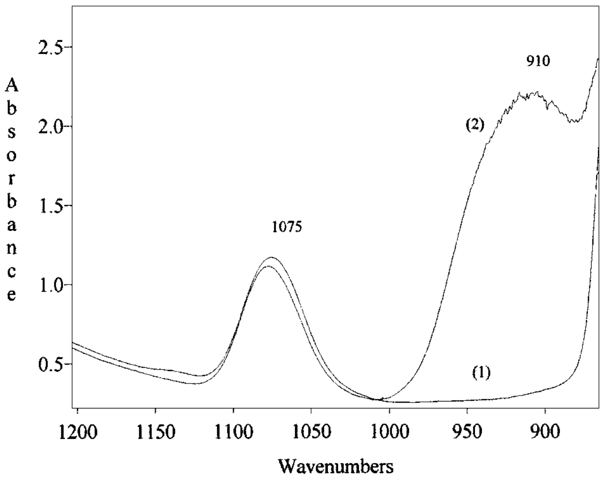

FIG. 2. IR spectrum of (1) catalyst precursor and (2) heated at 240°C in air for 4 h.

The formation of Cr=O as a function of time at 240°C is shown in Fig. 3. The dehydrated surface chromium oxide species present in chromium oxide/lanthanum carbonate catalysts differ from those observed on other supports such as Al_2O_3, TiO_2, and ZrO_2, in which the IR bands assigned to the symmetric stretching mode of Cr=O appear in a higher frequency region (16). The 908 cm^{-1} band obtained on this catalyst is typical of the presence of terminal CrO_3 units in CrO_3/SiO_2 catalyst (14) and $La_2(CrO_4)_3$ (17). The intensity of this band increases as the time of treatment is increased. This indicates that prolonged activation is needed in order to obtain high Cr=O concentrations when the catalyst is activated at 240°C or below. In oxidation reactions, the reactivity of the surface chromium oxide species is controlled

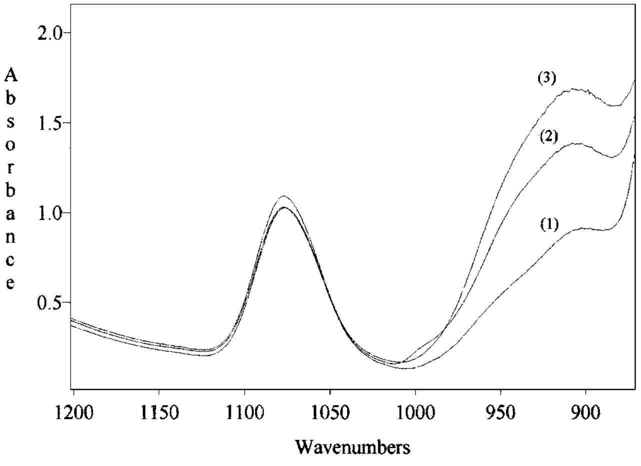

FIG. 3. Formation of Cr=O as a function of time at 240°C in air: (1) 30 min; (2) 1 h; (3) 2 h.

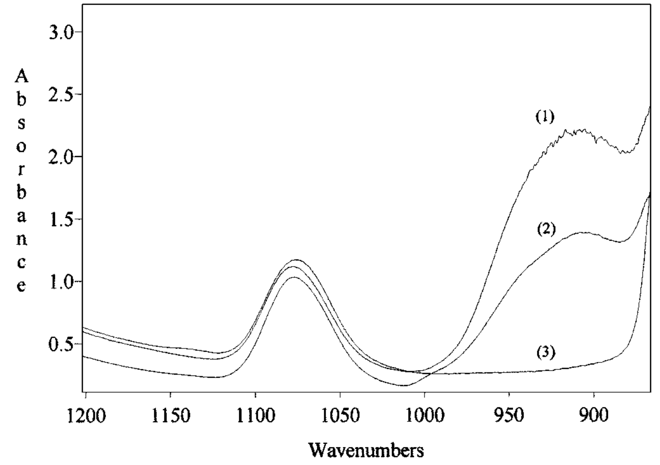

FIG. 4. IR spectrum of (1) activated catalyst, (2) exposed to 100 Torr isobutane at 240°C for 15 min, and (3) exposed to isobutane at 240°C for 1 h.

primarily by their molecular structure and the catalyst supports. Since the Cr—O–support bond is directly influenced by the acidity/basicity of the support, the energy of this bond is possibly the key to catalyst activity and selectivity.

In situ reduction/oxidation of the catalyst. After activation in air at 240°C for 2 h, the catalyst was exposed to isobutane at a pressure of 50 Torr at 240°C for 1 h. The intensity of the IR band at 908 cm^{-1} decreased markedly, as can be seen in Fig. 4. A complete reversibility is observed when the catalyst is reoxidized in air at 240°C. The catalytic results from the pulse reactor had indicated that the catalyst activity can be restored by exposure to oxygen at reaction temperature (6).

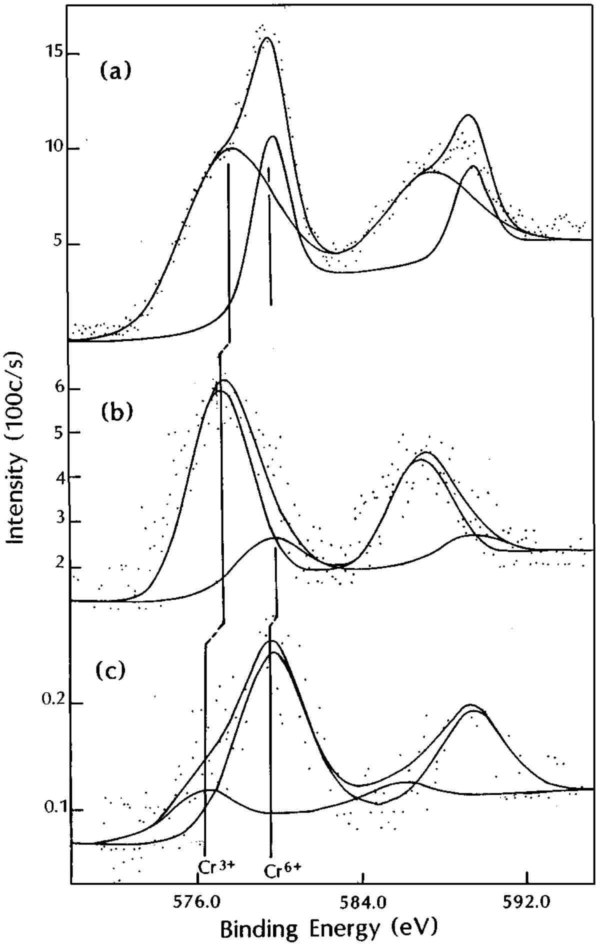

FIG. 5. Cr2*p* XPS spectra for supported chromium oxide/lanthanum carbonate: (a) 50, (b) 10, and (c) 5 mol% Cr_2O_3 loading.

X-Ray Photoelectron Spectroscopy

There have been several reports of XPS analyses for supported chromium oxide catalysts. Chromium in valence states of VI and III and in the metallic state can be distinguished by the difference in binding energy. In the present work, the XPS spectrum of the Cr2*p* of supported chromium oxide/lanthanum carbonate (Fig. 5) features two regions: One in the vicinity of 579.3 ± 0.3 eV and the other spread across the region 576.8 to 577.6 eV for 5 and 50% chromium oxide loading, respectively. The former is attributed to Cr(VI). In the later, a little more explanation is required. The catalyst preparation involves the thermal decomposition of $NH_4Cr(OH)_2CO_3$ at 300°C. An intermediate product of the decomposition is CrOOH. The binding energies of Cr_2O_3 and CrOOH are well known at around 576.6 and 577.7 eV, respectively (18). The lower binding energy Cr2*p* peak is broader for the 50% loading sample indicating the presence of both Cr_2O_3 and CrOOH. Thus, it is likely that at high loading level, the decomposition was not completed. No other valence states of chromium could be identified. Figure 5 and Table 1 show the results of XPS analysis for three catalysts with different chromium loadings. At low levels of chromium loading, 76% of chromium oxide is stabilized in the (VI) oxidation state after calcination in air at 240°C. At higher loading levels, the Cr(VI)/Cr(III) ratio was substantially lower. Unlike SiO_2, $La_2(CO_3)_3$ possesses lower surface area; thus, CrO_3 binds to the surface as a polymeric chromate species which possesses Cr=O terminals. When the temperature is raised, it is likely that unbound CrO_3, formed during the activation step, undergoes decomposition to give α-Cr_2O_3.

TABLE 1

XPS Analysis of Supported $Cr_2O_3/La_2(CO_3)_3$ Calcined in Air at 240°C

Cr loading[a]	Cr(III) (%)	Cr(VI) (%)	Cr/La	CO_3/La	O/Cr
5	24	76	0.10	1.02	35.5
10	74	26	0.13	0.93	44.0
50	73	27	0.99	0.64	4.7

[a] mol% (as Cr_2O_3).

Supported chromium oxide catalysts have been studied by many authors using XPS (19, 20), since they are effective for a number of commercially important reactions such as dehydrogenation, hydrogenation, and polymerization of olefins. Changes in oxidation state of chromium during heat treatment in different atmospheres have been the subject for many ESR, FTIR, and XPS studies. Attention has been given to the effect of the support textural features and the level of chromium addition.

The Cr(VI) binding energies of 579.3 and 579.6 eV for 10 and 50% Cr loading, respectively, are close to the value expected for CrO_3 (20, 21) and well within the range of Cr(VI) binding energies reported for supported chromium oxide catalysts. For example, Merryfield *et al.* (20) reported a value for Cr(VI) of 581.6 eV for chromium oxide/silica; Okamoto *et al.* (21) reported a $Cr2p_{3/2}$ value for chromium oxide/alumina of 579.7 eV; and similarly Cimino *et al.* obtained a binding energy of 579.7 eV for supported chromium oxide/zirconia catalysts (19). In the present work, for 5 mol% Cr loading level the binding energy of Cr(VI) was shifted to 578.8 eV, but this value still falls within the Cr(VI) regime. A binding energy of 578.4 eV for Cr(VI) was observed by Wachs *et al.* for a supported chromium oxide/alumina catalyst (22). The lower binding energy could well reflect a higher electron density on the Cr ion and possibly on the chromate group as a result of electron transfer from the basic lanthanum carbonate support to the adsorbed species. Alternatively, lower oxidation states have been hypothesized and observed in the literature and the shift to lower binding energy may reflect the presence of a lower oxidation state form of chromium. For example, the formation of Cr(V) and a binding energy of 577.8 eV has been reported by Okamoto *et al.* (21) for supported chromium oxide/alumina catalyst. This value is well below that observed for 5 mol% chromia/lanthanum carbonate catalyst. Moreover, this Cr(V) species is formed only under mild reduction or high-temperature evacuation of Cr(VI).

In contrast, Cr(VI) is the most stable valency state of chromium in oxidizing atmospheres. Since the catalysts have been activated in air, the shift to lower binding energy for the Cr(VI) on the catalyst containing 5 mol% loading is most likely due to a difference in metal–support interaction between chromium and lanthanum carbonate.

The Cr/La ratios obtained by XPS analysis for 5 and 10 mol% chromium loading samples are higher than that expected for the overall composition ratio of the catalyst suggesting that at low loading levels, most chromium is situated on the external surface of lanthanum carbonate. However at a 50% loading, the surface composition measured by XPS approached the overall composition ratio. The presence of oxygen from lanthanum carbonate imposed difficulties in quantifying the O/Cr ratio, particularly for catalysts with low chromium contents. However, at 50 mol% chromium loading, the surface O/Cr ratio as analyzed by XPS was 4.7 (Table 1) which is much closer to the expected value of 4 for chromate species.

The active phase for oxidative dehydrogenation is believed to be the surface oxide chromates in which chromium is chemically bound to the oxygen of the catalyst support. Depending on the loading level, the active phase can be chromate, dichromate, or more highly polymerized species with Cr═O terminals. The identification of similar species in the Phillips catalyst (CrO_3/SiO_2 for ethylene polymerization) has proven difficult and rather controversial. The most common agreement is that, after high-temperature activation, chromium is bound to the surface through water elimination between chromic acid and surface silanol. In the case of supported chromium oxide/lanthanum carbonate catalyst, the $CO_3^{=}$/La ratios obtained by XPS analysis were substantially lower than the expected value of 1.5 for lanthanum carbonate, indicating the interaction between chromium and the support surface through CO_2 elimination.

The effect of catalyst activation conditions is summarized in Table 2. Chromium in the catalyst precursor is present in a carbonato complex form of $NH_4Cr(OH)_2CO_3$; thus, chromium is stabilized in the (III) oxidation state. After high-temperature activation in oxygen, chromium is bound to the surface in the form of chromates shown by the appearance of a Cr(VI) peak at a binding energy of 579.3 eV. It is clear that the presence of oxygen in the activation step is necessary for the formation of chromates species since no Cr(VI) was detected by XPS on the catalyst after activation in argon. The Cr/La ratios in the activated catalyst were similar to those obtained for the precursor. No evidence of any transformation of Cr to the bulk phase such as binary oxide was observed, and the $CO_3^{=}$/La ratio was decreased upon heat treatment.

Changes in surface composition under reaction conditions have been studied at 250°C. The results are summarized in Table 3. Upon exposure to isobutane at 250°C, the reduction of Cr(VI) was observed. This is characterized by the appearance of a single peak at a binding energy of 577.3 eV. The catalyst can be regenerated at reaction temperature even with 1% O_2/He. After reduction/oxidation treatment an increase in Cr/La ratio was observed, suggesting that a redispersion of chromium on the surface had occurred. The CO_3/La ratios were virtually unchanged.

TABLE 2

Effect of Activation Conditions on the Formation of Active Phase

Treatment	Cr(III) (%)	Cr(VI) (%)	Cr/La	CO_3/La
Precursor	100	0	0.14	1.6
Ar, 300°C	100	0	0.13	1.1
1% O_2/He, 250°C	72	28	0.13	1.1

TABLE 3

Effect of Oxidation–Reduction Treatment

Treatment	Cr(III) (%)	Cr(VI) (%)	Cr/La	CO_3/La
Calc. air, 250°C	74	26	0.13	0.93
Isobutane, 250°C	100	0	0.16	1.11
1% O_2/He, 250°C	78	22	0.18	1.11

Electrophoretic Study

As chromium oxide in the activated catalyst is stabilized as Cr(VI) which is possibly soluble in water, the IEP of Cr(VI) oxide cannot be obtained by this technique. The IEP of the catalyst precursor, $NH_4Cr(OH)_2CO_3$, was measured and the ASC value was calculated based on a mixture composed of $NH_4Cr(OH)_2CO_3/La_2(CO_3)_3$. Figure 6 shows the Zeta potential as a function of the pH.

Both $La_2(CO_3)_3$ and $NH_4Cr(OH)CO_3$ are typical amphoteric materials which show an inversion of the polarization signal when the pH changes from acidic to basic region. The IEPs of $La_2(CO_3)_3$ and $NH_4Cr(OH)_2CO_3$ were 8.3 and 7.7, respectively. Although the surface of lanthanum carbonate polarizes positively at pH < 8.3, which indicates its adsorption capability for anions in a weak base medium, this becomes significant only at pH < 7.5. As expected, the ZPC of the $NH_4Cr(OH)_2CO_3/La_2(CO_3)_3$ mixture falls between the IEP of the individual components and decreases with increasing $NH_4Cr(OH)CO_3$ content. This is a result of an increase in the fraction of $La_2(CO_3)_3$ surface covered by chromium species. The results are summarized in Table 4.

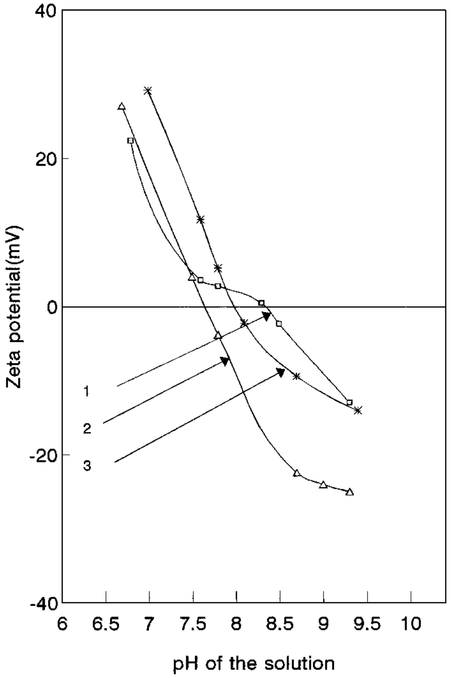

FIG. 6. Zeta potential as a function of pH. (1) $La_2(CO_3)_3$; (2) $NH_4Cr(OH)_2CO_3$; (3) catalyst precursor (25 mol% $NH_4Cr(OH)_2CO_3$/$La_2(CO_3)_3$).

TABLE 4

Zero Point Charge and Apparent Surface Coverage as a Function of Chromium Loading

Cr loading (%)[a]	IEP (pH)	ZPC (pH)	ASC (%)
0	8.4	—	—
5	—	8.1	21
10	—	7.9	47
25	—	7.7	100
50	—	7.7	100
$NH_4Cr(OH)_2CO_3$	7.7	—	—

[a] As mol% Cr_2O_3.

As the surface of $La_2(CO_3)_3$ is only 20 m^2/g, a full surface coverage was observed at chromium loading levels (as Cr_2O_3) > 25 mol%. The ASC values obtained by this technique indicate that chromium species are preferentially segregated at the external surface. Thus, high chromium loading levels will result in the formation of unreactive crystalline chromium oxide upon heating and subsequently lowering the overall activity of the catalyst.

CONCLUSIONS

The present combined FTIR and XPS studies reveals the formation of surface chromate species on the surface of lanthanum carbonate. The catalytic property of supported chromium oxide/lanthanum carbonate is due to surface chromium (VI) oxide species, not to bulk chromium oxide or $LaCrO_3$. The surface chromium (VI) oxide is bound to the surface, as at elevated temperatures bulk CrO_3 is no longer stable. Thus, both the nature of the support and the chromium content as well as the activation conditions will have an effect on the formation of active species. The presence of gaseous oxygen in the activation step is necessary to obtain maximum Cr=O concentration. The formation of these species is reversible during reduction–oxidation at 240°C. A full surface coverage was observed by electrophoretic analysis at chromium oxide loading >25%.

REFERENCES

1. Lugo, H. J., and Lunsford, J. H., *J. Catal.* **91**, 155 (1985).
2. Kim, D. S., and Wachs, I. E., *J. Catal.* **142**, 166 (1993).
3. Sun Company Inc., U.S. Patent 5,220,080 (1993).
4. Rohm and Haas Company, European Patent 0-520-779, A2 (1992).
5. McDaniel, M. P., *J. Catal.* **76**, 17 (1982).
6. Hoang, M., Mathews, J. F., and Pratt, K. C., *J. Catal.* **171**, 000 (1997).
7. Foger, K., Hoang, M., and Turney, T. W., *J. Mater. Sci.* **27**, 77 (1992).
8. Cumpson, P. J., and Seah, M. P., *Surf. Interface Anal.* **18**, 345 (1992).

9. Gil-Llambias, F. J., Escudey-Castro, A. M., and Bouyssieres-McLeod, L., *J. Catal.* **88**, 222 (1984).
10. Gil-Llambias, F. J., Escudey-Castro, A. M., Lopez-Agudo, A., and Gacia-Fierro, J. L., *J. Catal.* **90**, 323 (1984).
11. Gil-Llambias, F. J., Escudey-Castro, A. M., Lopez-Agudo, A., and Gacia-Fierro, J. L., *J. Catal.* **95**, 520 (1985).
12. Gil-Llambias, F. J., Rodriguez, H., Bouyssieres-McLeod, L., Escudey-Castro, A. M., and Carkovic, I., *J. Catal.* **102**, 37 (1986).
13. Cimino, A., Cordischi, D., Febbraro, S., Gazzoli, D., Indovina, V., Occhiuzzi, M., and Valigi, M., *J. Mol. Catal.* **55**, 23 (1989).
14. Zecchina, A., Garrone, E., Ghiotti, G., Morterra, C., and Borello, E., *J. Phys. Chem.* **79**(10), 966 (1975).
15. Indovina, V., Cordischi, D., De Rossi, S., and Ferraris, G., *J. Mol. Catal.* **68**, 53 (1991).
16. Vuurman, M. A., Wachs, I. E., Stufkens, D. G., and Oskam, A., *J. Mol. Catal.* **80**, 209 (1993).
17. Okamoto, Y., Adachi, K., Imanaka, T., and Teranishi, S., *Chem. Lett.* 241 (1974).
18. Desimoni, E., Malitesta, C., Zambonin, P. G., and Riviek, J. C., *Surf. Interface Anal.* **13**, 173 (1988).
19. Cimino, A., Cordischi, D., De Rossi, S., Ferraris, G., Gazzoli, D., Indovina, V., Minelli, G., Occhiuzzi, M., and Valigi, M., *J. Catal.* **127**, 744 (1991).
20. Merryfield, R., McDaniel, M., and Parks, G., *J. Catal.* **77**, 348 (1982).
21. Okamoto, Y., Fujii, M., Imanaka, T., and Teranishi, S., *Bull. Chem. Soc. Jpn.* **49**(4), 859 (1976).
22. Vuurman, M. A., Hardcastle, F. D., and Wachs, I. E., *J. Mol. Catal.* **84**, 193 (1993).